Berkala **PENELITIAN HAYATI**

ISSN: 08526834 | E-ISSN:2337-389X

Volume 31 | No. 1 | **April** | 2025

Original article

In-Silico molecular docking analysis of monoclonal antibodies, approved inhibitors, and plant-based inhibitors targeting extracellular and intracellular HER2 receptor

Harish Hakaman[1], Felice Surya[1], Gizella Els Gerardine[2], Hanny Honggo[1], Arli Aditya Parikesit[3*]

[1] Department of Biotechnology, School of Life Sciences, Indonesia International Institute of Life Sciences, Jakarta, Indonesia
[2] Department of Biomedicine, School of Life Sciences, Indonesia International Institute of Life Sciences, Jakarta, Indonesia
[3] Department of Bioinformatics, School of Life Sciences, Indonesia International Institute of Life Sciences, Jakarta, Indonesia

Abstract

Human epidermal growth factor receptor or HER2 is a key player in breast, ovarian, and gastric cancers. Mutations that cause HER2 overexpression may alter their binding properties and sensitivity towards certain drugs. This study investigates the sequential amino acid interactions of extracellular HER2 receptors with antibodies and intracellular HER2 receptors with chemical inhibitor ligands using Molecular Docking to obtain the best drug model with the greatest binding affinity to the HER2 receptor. Additionally, analysis of the HER2 protein-protein interactions, degradation mechanism, stability analysis, Lipinski's Rule of Five, ADMET profiling of the inhibitors was done. The molecular docking of extracellular HER2 receptor and antibodies Trastuzumab and Pertuzumab showed higher binding affinity for the improved Trastuzumab. Molecular docking of intracellular HER2 receptor and 12 inhibitor ligands showed that the binding affinity of the plant-based inhibitor was not higher than the control inhibitor, SYR127063. However, the opposite goes for the approved inhibitors Tucatinib and Lapatinib, as it gives a higher binding affinity than control. According to Lipinski's Rule of Five, ADMET profile and molecular docking results, the best-approved inhibitors and plant-based inhibitors were Lapatinib and Sanguinarine, respectively. Although Lapatinib's MW exceeds 500 g/mol, violating Lipinski's drug likeness parameter, and Sanguinarine's protein-ligand stability analysis proved unstable, while Dacomitinib is the most stable. The results provided information on the binding properties of HER2 receptors with various inhibitors, which could be useful for future research on potential anti-cancer drugs to target and degrade HER2 receptors with optimal binding affinity. Furthermore, *in-vitro* cell-based assay studies are required to test the efficacy of the plant-based inhibitors toward HER2 receptor and cellular safety.

Keywords: Approved inhibitor, HER2ex, HER2in, plant-based inhibitor, Pertuzumab, Trastuzumab
Received: December 16, 2024 Revised: January 21, 2025 Accepted: January 27, 2025

Introduction

HER2 protein role in numerous cancers

Human epidermal growth factor receptor 2 (HER2), commonly referred to as ERBB2 and a member of the epidermal growth factor receptor (EGFR) family, is a critical player in the initiation and progression of numerous types of cancer, including breast, ovarian, and gastric cancers (Arienti et al., 2019; Jakhmola et al., 2022). Overexpression of HER2, often resulting from mutations in the HER2 gene, leads to uncontrolled cell growth and division, promoting the development and progression of cancer (Galogre et al., 2023; Parikesit et al., 2024). These mutations can produce mutated HER2 receptors, altering their binding properties for ligands and potentially increasing sensitivity to certain drugs. This overexpression is often associated with poor prognosis in cancer patients, making it a prime target for therapeutic intervention (Gaibar et al., 2020). Furthermore, HER2 signaling can promote cell survival by inhibiting apoptosis, enabling cancer cells to evade programmed cell death signals and persist within the tumor microenvironment (Rahman et al., 2022; Zhang et al., 2024). HER2 activation stimulates angiogenesis, fostering the formation of new blood vessels to sustain tumor growth and metastatic dissemination (Alifiansyah et al., 2024; Zhou et al., 2021). In addition, HER2-positive cancers exhibit enhanced invasiveness and metastatic potential, facilitated by HER2-mediated induction of epithelial-to-mesenchymal transition, enabling cancer cells to invade surrounding tissues and disseminate to distant sites (Zimmer et al., 2020). HER2-driven cancers may resist targeted therapies, compromising treatment efficacy and contributing to disease progression (Goutsouliak et al., 2019).

* Corresponding Author:
Arli Aditya Parikesit
Department of Bioinformatics, School of Life Sciences, Indonesia International Institute of Life Sciences, Jakarta, Indonesia
Phone: +622129567888
E-mail: arli.parikesit@i3l.ac.id

Molecular mechanism and genomics of HER2 ligand binding

The molecular mechanism of HER2 ligand binding involves a complex interplay of protein-protein interactions and conformational changes. HER2 lacks a known ligand-binding domain and can form heterodimers with other HER family members, such as HER1 (EGFR), HER3, and HER4 (Kumar et al., 2020). Ligand binding to HER2 heterodimers induces receptor activation through dimerization and autophosphorylation of tyrosine residues in the intracellular domain. This activation triggers downstream signaling cascades, including the PI3K/AKT and MAPK pathways, which regulate cell proliferation, survival, and differentiation (Cordover and Minden, 2020; Widyananda et al., 2021).

http://dx.doi.org/10.23869/bphjbr.31.1.20256
Published by © PBI East Java. Open Access www.berkalahayati.org

Genomic studies have revealed the genetic alterations contributing to HER2 activation and signaling dysregulation in cancer cells, including amplifications, mutations, and rearrangements.

Understanding the molecular mechanisms and genomics of HER2 ligand binding is essential for developing targeted therapies aimed at disrupting HER2 signaling and improving clinical outcomes in HER2-positive cancers (Ansori et al., 2024). Thus, to identify active site sequential amino acid interactions of extracellular HER2 receptor with antibody inhibitor, and intracellular HER2 receptor with ligand inhibitor, to obtain the best drug model with the best cluster model with the highest binding affinity to modulate greatest inhibition. Determining the best intracellular HER2 ligand to be suitable for incorporation into the human body through ADMET profiling. Discovering the HER2 protein-protein partner can help identify the downstream response upon HER2 inhibition.

Methods

Structural data collection

Firstly, data was collected for structural analysis. The RCSB database was used to identify and obtain the structure in .pdb format for the extracellular domain of HER2 receptor (HER2ex) (PDB ID: 6OGE 4.36Å, extracellular HER2 domain-Trastuzumab Fab-Pertuzumab Fab complex), and intracellular domain of HER2 receptor (HER2in) (PDB ID: 3PP0 2.25Å, Kinase domain of Human HER2 (ERBB2) complexed with SYR127063 inhibitor ligand) (Burley et al., 2022). Additionally, the structure of antibodies that were able to interact and inactivate HER2 to target HER2ex were also collected, which are improved Trastuzumab (PDB ID: 4HJG 2.00Å, Meditope-enabled Trastuzumab) and improved Pertuzumab (PDB ID: 4LLW 1.95Å, Pertuzumab Clambda Fab with variable domain redesign (VRD2)).

In this study, a total of 12 combined approved and plant-based ligand inhibitors shown by previous studies were used (Akinnusi et al., 2022; Arsianti et al., 2023; Collins et al., 2019; Hermanto et al., 2017; Perumal et al., 2015; Pradubyat et al., 2021; Tung et al., 2023; Wang et al., 2022; Yang et al., 2024). To obtain the 3D conformer of these selected inhibitors, PubChem was used; these approved inhibitors include Dacomitinib, Lapatinib, Neratinib, Pyrotinib, Tucatinib, and Capecitabine, while the plant-based inhibitors known to interact with HER2in are Coptisine (from *Coptis chinensis*), Sanguinarine (from *Sanguinaria canadensis*, *Argemone mexicana*, *Chelidonium majus* and *Macleaya cordata*), Gallic Acid (from a range of various fruits, plants and nuts), Peonidin-3-glucoside (from *Vitis vinifera*, red *Allium cepa* and purple *Zea mays*), 1'-Acetoxychavicol acetate (from *Alpinia galanga* and *Alpinia conchigera)*, and 4,8,12,16-Tetramethylheptadecan-4-olide (from various plants, but notably from *Millettia speciosa* and *Deinbollia pinnata*).

Receptor and ligand structure modification

After acquiring the structures, the HER2ex non-standard residues (NAG, MAN, and BMA ligand) were removed. The Trastuzumab and Pertuzumab complexes were also removed, in which the Trastuzumab and Pertuzumab structures were used as control antibodies. Using the ChimeraX application, the clean HER2ex structure was used as the antigen for antibody docking, and the removal of HER2in non-standard residues, was done while using the SYR127063 ligand as its control to obtain a clean HER2in (Paul et al., 2024). Both HER2ex and HER2in were further modified by removing the water molecule, repairing the missing atoms, adding the polar hydrogen molecule, applying Kollman charges to remove unwanted docking targets, and assigned as AD4 type. These modifications were also applied to 4HJG and 4LLW test antibodies using AutodockTools:MGLTools (Pawar et al., 2023).

All the approved plant-based ligand inhibitors were added with hydrogen and converted to .pdb format using the Avogadro2 application to be docked with HER2 (Raubenolt and Blankenberg, 2024).

Molecular docking of antibody-HER2ex and ligand-HER2in Complexes

Molecular docking of HER2ex was done using ClusPro 2.0 in which the antigen of HER2ex was set as the receptor. The control antibody and test antibody acted as the ligand with the process being carried out based on blind docking (Kozakov et al., 2017). Afterward, the obtained antibody-receptor complex results must have the correct Trastuzumab (binds to subdomain IV of HER2ex) and Pertuzumab (binds to subdomain II of HER2ex) binding location; this was done through the calculation of cluster scores in the center and lowest energy based on the balanced coefficient weights made by the ClusPro 2.0. Coefficient weights represented by $[E = w1Erep + w2Eatt + w3Eelec + w4EDARS]$ is to calculate interaction energies between proteins In the formula, *Erep*, *Eatt*, *Elec*, *and EDARS* represent the repulsive van der Waals energy, attractive van der Waals energy, electrostatic energy, and desolvation energy, respectively, which is set by the ClusPro 2.0 upon docking. In ClusPro 2.0, a PIPER docking algorithm is used for protein sampling. During the sampling, the receptor protein is fixed at the origin and the ligand is evaluated through rotations on a spherical grid with 70,000 possible rotations, and translated with a step size of 1 Ångström (Kozakov et al., 2017).

Molecular docking of HER2in was performed using PyRx (Trott and Olson, 2009) by first loading the modified HER2in molecule 3PP0, marking it as macromolecules or receptors, and converting it to .pdbqt format. Through the PyRx's openbabel tab, all six approved, six plant-based inhibitors, and the SYR127063 control inhibitor ligand were inputted, energy-minimized to apply steepest descent algorithm and Universal Force Field to the ligands (Paul et al., 2025), and converted to Autodock ligand (.pdbqt) format. The grid parameters derived from the visualization of SYR127063 location in

BIOVIA were located at 35 center_x, 46 center_y, and -12 center_z, and this binding location was visualized using Discovery Studio BIOVIA, where SYR127063 binds in subdomain II (Yahaya et al., 2021). Thus, the gridbox parameter of 35 center_x, 46 center_y, -12 center_z, and the same 35 size_x, size_y, and size_z for a consistent targeted active site docking, along with the exhaustiveness of 20 for a more thorough space search was set and run (Che and Zhang, 2023). As a result, the binding affinity for each ligand was recorded, the best results were noted, and re-docking was performed two more times to ensure accurate results and the reliability of the PyRx software by calculating the standard deviation of three total runs.

Visualization of antibody-HER2ex and ligand-HER2in complexes' molecular docking results

To visualize the molecular docked antibody-antigen complexes, the best model files were downloaded from Cluspro 2.0 and uploaded in the PDBsum website "generate" section. The structure residue interaction and visualization were retrieved from PDBsum's protein-protein interaction and PyMOL on the website (Desta et al., 2023).

On the other hand, to visualize the molecular docked protein-ligand complexes, the best model files were downloaded from PyRx with the highest binding affinity and uploaded to Discovery Studio BIOVIA to identify the residue interaction.

Molecular dynamics of ligand-HER2in stability analysis

A molecular dynamics simulation of the docked HER2in protein-inhibitor ligand complex was performed using the CABSflex 2.0 website to evaluate conformational changes and binding stability (Dibha et al., 2022). For all the 13 simulations, all parameters including distance restraint generator, additional distance restraints, and advanced simulation options were maintained at their default settings (Aurora et al., 2022; Khan et al., 2024).

Lipinski's Rule of Five

Lipinski's Rule of Five's analysis was done through inputting the SMILES format of the control, approved, and plant-based inhibitor ligand to the SWISS-adme website. The generated result, which includes molecular weight, number of hydrogen bond donors and acceptors, consensus lipophilicity Log$P_{o/w}$, and Lipinski's drug likeness and possible violations were noted.

ADMET profiling

ADMET profiling of all 12 viable ligands was done by first taking the .sdf format of each ligand from PubChem. Then, the file is converted into SMILES format to fit into the input needed for pkCSM tool (Herdiansyah et al., 2024).

pkCSM tool predicts the pharmacokinetic properties and determine how well the body will react to the drug (Hamami et al., 2022). Specifically, the absorption, distribution, metabolism, excretion, and toxicity were measured through 30 different parameters; though, only 10 parameters were taken and analyzed for this research: CACO3 permeability, intestinal absorption, VDss, metabolism of CYP2D6, CYP3A4, CYP2D6, and CYP3A4, total clearance, AMES toxicity, and hepatotoxicity. The software functions by calculating 341 molecular descriptors that will predict the drug reaction, and it also validates the prediction using another set of already predicted drugs (El-Saadi et al., 2015).

HER2 functional protein-protein partners identification

Functional Protein-protein Partners Identification of HER2 (ERBB2) protein was done by inserting the "ERBB2" name into the STRING database to identify the scores of functional protein-protein partners and their association.

Results and Discussion

Extracellular HER2 receptor molecular docking analysis

The HER2ex protein analysis revealed significant binding interactions between HER2 and the four selected antibodies. The improved Trastuzumab version (PDB ID: 4HJG) showed a more negative center and the lowest binding energy with HER2ex compared to the control Trastuzumab. Meanwhile, the control Pertuzumab version demonstrated more significant interactions and lower cluster scores than the improved Pertuzumab (PDB ID: 4LLW).

The obtained formula was $[E = 0.40Erep + -0.40Eatt + 600Eelec + 1.00EDARS]$, which determine four main scoring schemes: balanced, electrostatic-favored, hydrophobic-favored, and van der Waals + electrostatic. For the specific parameter details, $w1$ and $w2$ were set to values less than 1.0 to soften van der Waals terms, $w3$ was set to 600 to balance the electrostatic measurements after smoothing, and $w4$ was set to 1.0 as the default for desolvation. These weights ensure the optimization success for cluster scores of different proteins (Kozakov et al., 2017).

The cluster scores of the control and improved molecules for both Trastuzumab and Pertuzumab docked to the HER2ex subdomains are compared to identifying the best version of the monoclonal antibody. Trastuzumab and Pertuzumab ClusPro 2.0 model structure chosen are based on the binding locations of Trastuzumab toward subdomain IV of HER2ex (Cavallaro et al., 2023), while Pertuzumab toward subdomain II of HER2ex (Cruz et al., 2023).

Table 1. Cluster Scores and Coefficient Weights of HER2ex and antibodies molecular docking results

Antibody	Docked molecule	Cluster Scores	
		Center	Lowest Energy
Trastuzumab	HER2ex-trastuzumab (control)	-786.5	-873
	HER2ex-Improved trastuzumab (ID: 4HJG)	-862.7	-1024.9
Pertuzumab	HER2ex-pertuzumab (control)	-1054.7	-1054.7
	HER2ex-Improved pertuzumab (ID: 4LLW)	-763.5	-784.3
Coefficient Weights:	$E = 0.40Erep + -0.40Eatt + 600Eelec + 1.00EDARS$		

As explained in Table 1, trastuzumab, its improved version (HER2ex-ImproTras) shows center and lowest energy scores of -862.7 and -1024.9 in their cluster scores, which is more negative than its Trastuzumab control which gives off -786.5 and -873.0. Thus, the improved antibody will provide a higher binding affinity than the control. However, the improved Pertuzumab resulted in higher cluster scores depicted by the center and lowest scores of -763.5 and -784.3 compared to both scores of -1054.7 in the control Pertuzumab.

Trastuzumab is a monoclonal antibody that binds to the extracellular subdomain IV of HER2. In order to mediate Trastuzumab binding and mechanism, epitope-binding regions of Trastuzumab's both light chain and heavy chain are required to bind to extracellular subdomain IV of HER2 (Boix-Perales et al., 2014). According to Zhao et al. (2021), upon Trastuzumab binding to HER2, it can acts as a dual role of antagonist of which inhibits HER2 dimerization with other family receptors, and agonist that leads to structural changes in the tyrosine kinase domain of dimerized HER2 state, which causes the change of ligand-induced phosphorylation molecules in the intracellular HER2 domain. The residues that are crucial for the interaction between Trastuzumab and HER2 receptors are Arginine, Isoleucine, Tyrosine, Proline, Threonine, Asparagine, and Glutamine (Cavallaro et al., 2023). A crystallography analysis of extracellular HER2 subdomain IV by Peng et al. (2023) found that Trastuzumab mediate HER2ex IV binding through the interaction with three regions loop of C-terminal part, in which the first region is from amino acid residues 557-561, the second region from 570-573, and the third region from 593-603. The first and third loop has electrostatic interactions, whereas the second region has mostly hydrophobic interactions. Another research by (Hermanto et al., 2017) predicted a crystal structure of complex HER2-Fab, whose residue has contacted the binding site at Trp99 that interacts with Phe573 by hydrophobic interactions. Hydrogen bonding between Asn30, Tyr92, Thr94, Arg50 and Gly103-Gln602, Lys569, Asp560, Glu558, Asp560 and Lys593, and ionic interactions in the Asp560 residues Arg59 and Arg50 with Glu558 and Asp560.

In A=D chains of Control HER2ex-Trastuzumab (Figure 1), the hydrogen bond residues in chain A were from Gln533, Val555, Arg558, Ser573, and Gln583. In A=E chains, the hydrogen bond residues in chain A were from Gly572, Ser573, and Lys591. Meanwhile, salt bridges were in Lys591(2), Glu619, and Glu620. Across

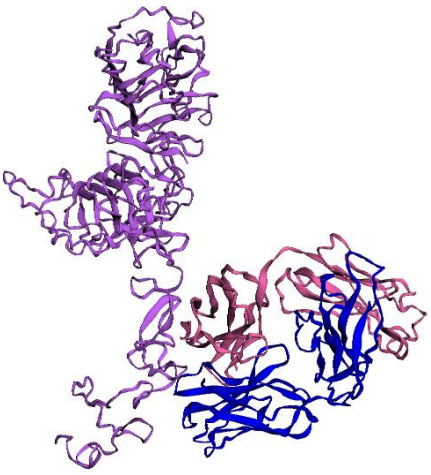

Chains	No. of interface residues	Interface area (A^2)	No. of salt bridges	No. of disulphide bonds	No. of hydrogen bonds	No. of non-bonded contacts
A-D	14:11	535:586	-	-	5	74
A-E	9:9	469:430	4	-	3	66

Figure 1. Control HER2ex-Trastuzumab interaction residues and visualization (PDBsum ID: vpo9). Chain A is HER2ex, chain D & E is Trastuzumab light and heavy chain.

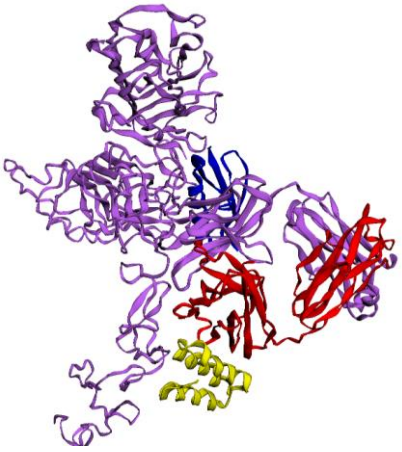

Chains	No. of interface residues	Interface area (A^2)	No. of salt bridges	No. of disulphide bonds	No. of hydrogen bonds	No. of non-bonded contacts
A-B	62:51	2520:2651	3	-	35	419
A-E	31:25	1346:1346	4	-	26	200
A-H	12:7	367:421	3	-	6	40

Figure 2. HER2ex-improved Trastuzumab interaction residues and visualization (PDBsum ID: vpo8). Chain A is HER2ex, chain B is heavy chain Trastuzumab, chain E is protein L fragment and chain H is immunoglobulin G-binding protein A.

all chain interactions, a very high amount of non-bonded contacts was generated. (2), (3), (4), etc. represent the occurrence of residue interaction.

In A=B chains of HER2ex-improved Trastuzumab (Figure 2), the hydrogen bond residues in chain A were from Ser532, Gln533 (2), Glu543 (2), Val555 (2), Tyr36, Gln38 (2), Ser43, Tyr49, Tyr55 (2), Tyr87, His91 (2), Thr93, Thr94, Val115, Ile117, Pro120, Asn137, Gln160 (3), Ser162, Ser174 (2), Lys207 (3), Ser208, Glu213, and Cys214. Meanwhile, salt bridges were in Asp122, Glu123, and Glu213. Meanwhile in A=E chains of HER2ex-Improved Trastuzumab (Figure 2), the hydrogen bond residues in chain A were from Gln24, Asn259 (2), Pro285, Arg288, (4) Ser294, Ala298, Ser7, Ile9, Leu10, Ser12 (2), Gly16, Asp17, Arg18 (5), Thr20,

Arg24, Ser67, and Lys107. The salt bridges were in Arg288, Asp326, Asp17, and Arg24. In A=H chains, the hydrogen bond residues in chain A were from Gln570, Asp582, Cys584, Lys591, and Glu619 (2) whereas the salt bridges were located in Lys591, Glu619, and Glu620. Across all chain interactions, a very high amount of non-bonded contacts was generated. (2), (3), (4), etc. represent the occurrence amount of residue interaction.

Pertuzumab is a HER2es dimerization inhibitor that binds to the extracellular subdomain II of HER2es. To mediate Pertuzumab binding and mechanism, epitope-binding regions of Pertuzumab's both light chain and heavy chain are required to bind to extracellular subdomain II of HER2 (Boix-Perales et al., 2014). The amino acid residue interaction is between the Phe257 residue of extracellular HER2es subdomain II and the Ile58, Tyr59, and Gln61 residues of the Pertuzumab heavy chain Fab (binding sites that can interact with HER2ex). There is a nonpolar-polar interaction between Gln61 and Phe257, and two nonpolar-nonpolar interactions between Ile58-Tyr29 and Phe257. These interactions arise from the proximity of the residues (Cruz et al., 2023). Non-covalent interactions such as hydrogen bonding between Ser310 of HER2ex and Asp31 of Pertuzumab play a major role in the tight binding of Pertuzumab and HER2ex (Zhang et al., 2019).

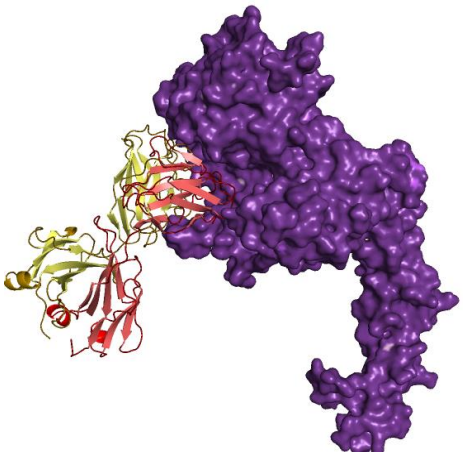

Chains	No. of interface residues	Interface area (A^2)	No. of salt bridges	No. of disulphide bonds	No. of hydrogen bonds	No. of non-bonded contacts
A⌘B	24:21	995:1054	2	-	11	129
A⌘C	16:23	971:824	1	-	10	113

Figure 3. Control HER2ex-Pertuzumab interaction residues and visualization (PDBsum ID: vpp1). Chain A is HER2ex, and chain B & C is Pertuzumab light and heavy chain, respectively.

In A=B chains of Control HER2ex-Pertuzumab (Figure 3), the hydrogen bond residues in chain A were from Lys150 (2), Asn177 (2), Arg351, Thr312, Ser310, Thr306, Leu317, and Gln81. Meanwhile, salt bridges were in Glu348 and Arg351. Meanwhile in A=C chains of Control HER2ex-Pertuzumab (Figure 3), the hydrogen bond residues in chain A were from Glu238 (3), His267, Asn176 (2), Asn177, Asp277 (2), Val272. One salt bridge was in Lys175. Across all chain interactions, a very high amount of non-bonded contacts was generated. (2), (3), (4), etc. represent the occurrence amount of residue interaction.

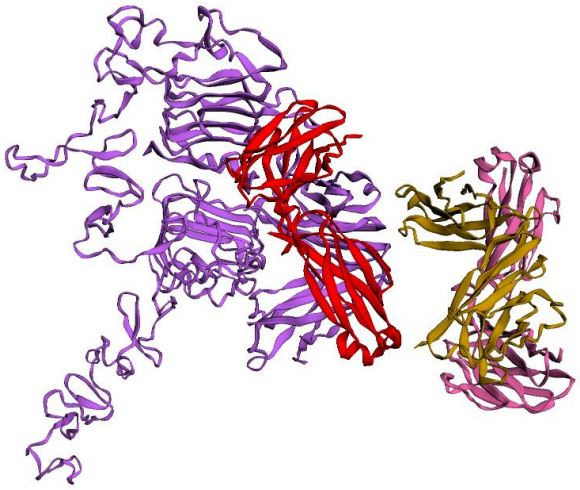

Chains	No. of interface residues	Interface area (A^2)	No. of salt bridges	No. of disulphide bonds	No. of hydrogen bonds	No. of non-bonded contacts
A⌘B	54:41	2075:2281	4	-	23	321
A⌘C	8:7	268:312	-	-	5	45

Figure 4. HER2ex-improved pertuzumab interaction residues and visualization (PDBsum ID: vpo7). Chain A is HER2ex, chain B is light chain clambda, and chain C is fab heavy chain mutated pertuzumab

In A=B chains of HER2ex-improved Pertuzumab (Figure 4), the hydrogen bond residues in chain A were from Lys32, His88 (2), Glu109, Arg157 (3), Tyr60, Lys65, Tyr95, Phe104, Phe106, Asp107, Tyr108 (2), Lyr149 (2), Asp150, Val169, Pro173, Ser185, and Lys215 (2). Meanwhile, salt bridges were in Glu109, Asp384, Asp150, and Lys215. In A=C chains of HER2ex-improved Pertuzumab (Figure 4), the hydrogen bond residues in chain A were from Gly66 (2), Ser85, and Arg87 (2). Across all chain interactions, a very high amount of non-bonded contacts was generated. (2), (3), (4), etc. represent the occurrence amount of residue interaction. Although previously, the control Pertuzumab offers a more negative or stronger binding affinity, Improved Pertuzumab shows a wider array of interactions, comprising 4 salt bridges and 23 hydrogen bonds. These docking results of HER2ex-Pertuzumab or Trastuzumab offer a new binding profile compared to the existing literature.

Intracellular HER2 receptor molecular docking analysis

Table 2. Molecular docking result of control inhibitor ligand and HER2in

No.	Compound name	Binding affinity to HER2in (kcal/mol)	SD (±)
1	SYR127063	-11.0	0.058

The molecular docking analysis of the control compound SYR127063 with the intracellular HER2 receptor reflected in Table 2, demonstrated a binding affinity of -11.067 kcal/mol with a very low standard deviation (SD) of 0.058. This binding affinity indicates a strong interaction between the control compound and the HER2in receptor, which could be crucial for inhibiting the HER2-related signaling pathways involved in cancer progression.

Table 3. Molecular docking result of approved and plant-based inhibitor ligand with HER2in

Rank	Type of HER2in inhibitor	Compound name	Binding affinity to HER2in (kcal/mol)	SD (±)
1	Approved	Tucatinib	-11.9	0.058
2	Approved	Lapatinib	-11.4	0.058
3	Approved	Pyrotinib	-10.9	0.1
4	Plant	Coptisine	-10.7	0.058
5	Plant	Sanguinarine	-10.6	0
6	Approved	Dacomitinib	-9.9	0.115
7	Approved	Neratinib	-9.8	0.173
8	Plant	Peonidin-3-glucoside	-9.5	0.252
9	Approved	Capecitabine	-8.1	0.115
10	Plant	4,8,12,16-tetramethylheptadecan-4-olide	-7.7	0.115
11	Plant	1'-Acetoxychavicol acetate	-7.1	0.1
12	Plant	Gallic acid	-7	0

The targeted docking toward the docking site HER2in subdomain II (Refer to Figure 5) shows a highly consistent binding affinity result and reliable molecular docking parameter are demonstrated in all control, approved, and plant-based ligands as seen in Table 3, judging by a low variability of the three PyRx molecular docking runs of around 0-0.252 SDs upon re-docking using the same grid parameter (Deepasree and Subhashree, 2023).

Notably, Tucatinib exhibited the strongest binding affinity with a score of -11.833 kcal/mol, followed closely by Lapatinib at -11.467. These inhibitors show higher affinity than the SYR127063 control, suggesting a stronger inhibition effect. Even though the plant-based inhibitor Coptisine and Sanguinarine value is lower than the control, it can be considered as a new plant-based inhibitor as it shows -10.767 and -10.6 kcal/mol binding affinity respectively, only around 0.3 and 0.4 difference with the control. Additionally, it demonstrates a higher affinity than other approved inhibitors of Dacomitinib at -9.967 kcal/mol, Neratinib at -9.9 kcal/mol, and Capecitabine at -8.067. As for the other inhibitor, Pyrotinib showed -10.9 kcal/mol. Other plant-based ligands such as Peonidin-3-glucoside and 4,8,12,16-Tetramethylheptadecan-4-olide showed binding affinities of -9.5 kcal/mol and -7.7 kcal/mol, respectively. The lowest binding affinity was shown by 1'-Acetoxychavicol acetate and Gallic Acid of -7.1 kcal/mol, and -7.0 kcal/mol, respectively (refer to Table 3). Hence, the top two approved and plant-based inhibitors will be further assessed in more detail.

The binding affinity with the most negative score other than the control, Lapatinib, is compound Tucatinib. A more negative score indicates less free energy in the binding, which shows a more favorable and stable binding (Pantsar and Poso, 2018). Hence, Tucatinib is an ideal ligand for the binding of HER2 receptors. Additionally, other approved inhibitors (compounds 3 to 6) are shown to have a higher binding affinity score than plant-based inhibitors (compounds 7 to 12). This demonstrates that the hypothesis confirmed by other journals, which states that the binding affinity of the best plant-based inhibitor should be higher than the control inhibitor, is unachieved.

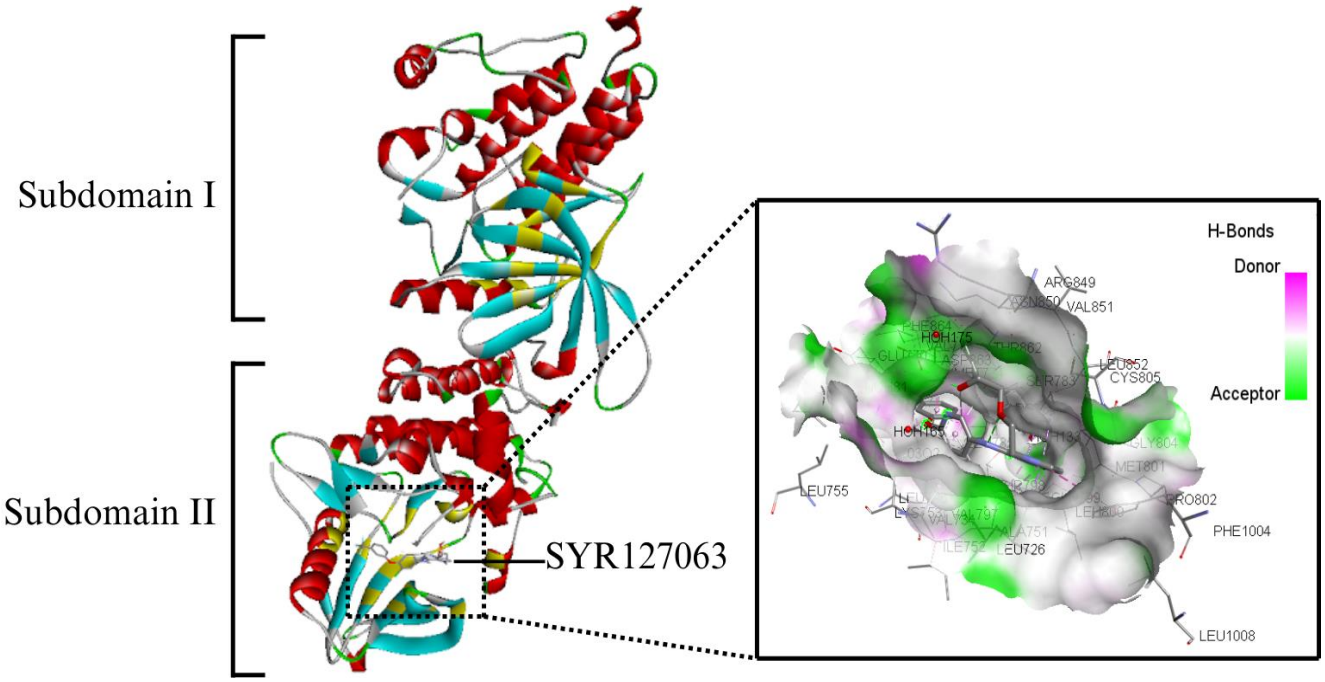

Figure 5. Visualization of 3PP0, HER2in structure containing SYR127063 binding subdomains. Subdomain II is the main docking site for inhibitor ligands, including the control ligand SYR127063. The yellow-colored residue is the binding amino acid.

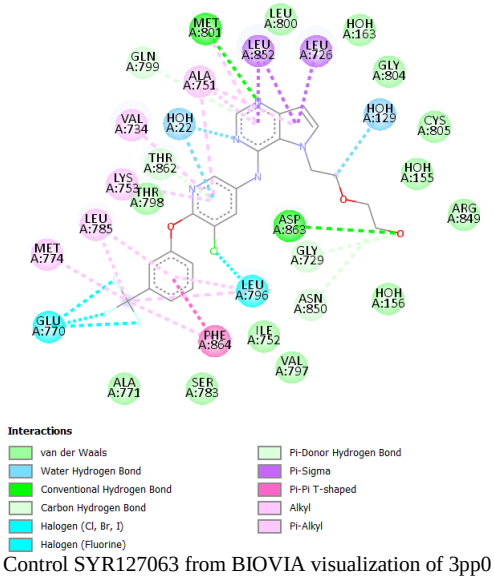

Control SYR127063 from BIOVIA visualization of 3pp0

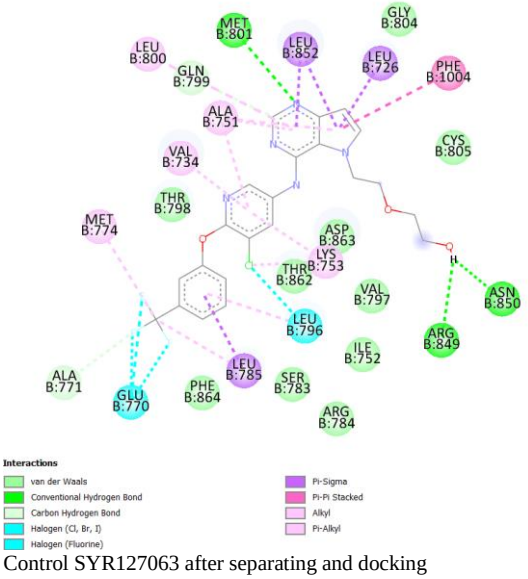

Control SYR127063 after separating and docking

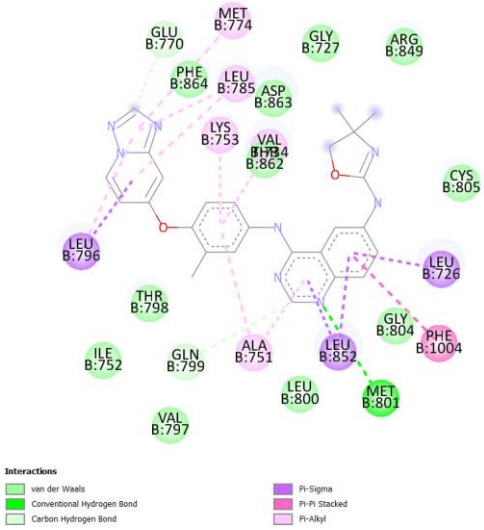

Rank 1:
Tucatinib docked residue

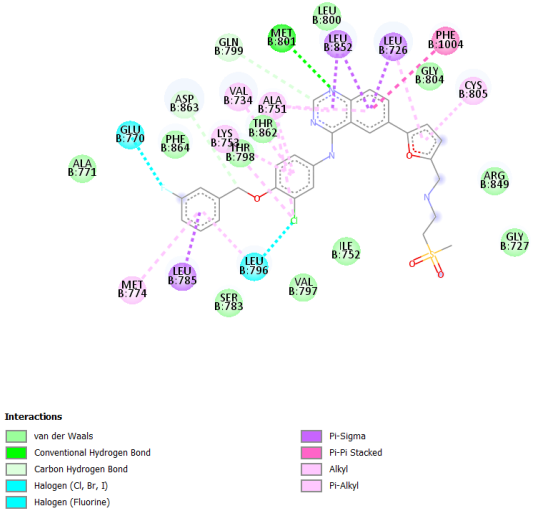

Rank 2:
Lapatinib docked residue

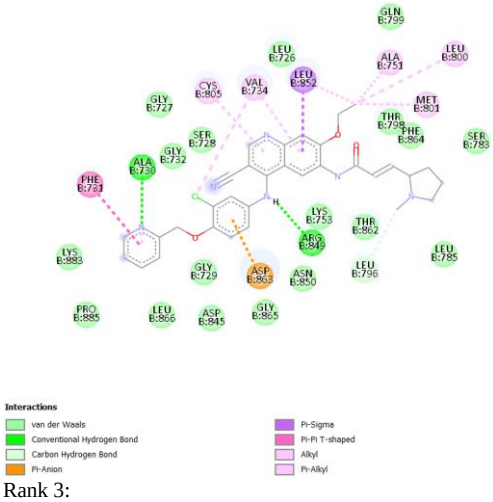

Rank 3:
Pyrotinib docked residue

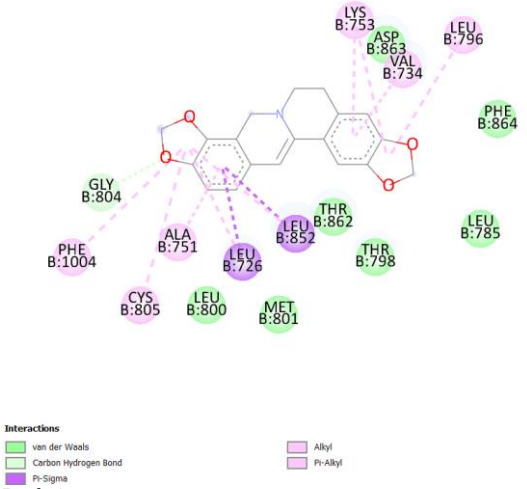

Rank 4:
Coptisine docked residue

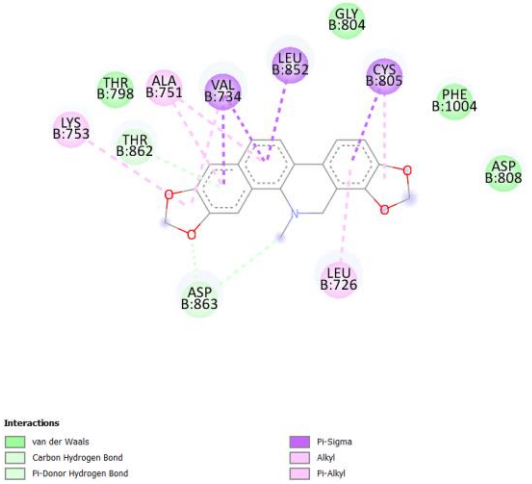

Rank 5:
Sanguinarine docked residue

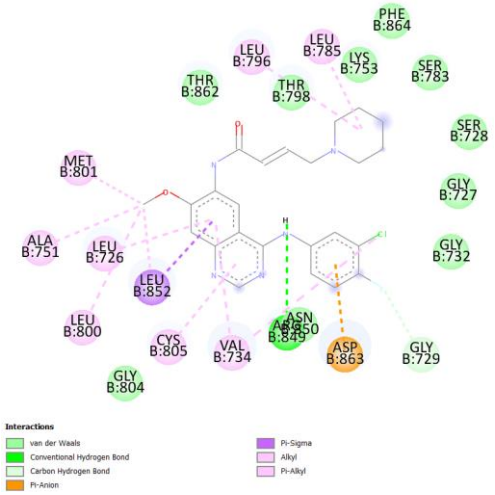

Rank 6:
Dacomitinib docked residue

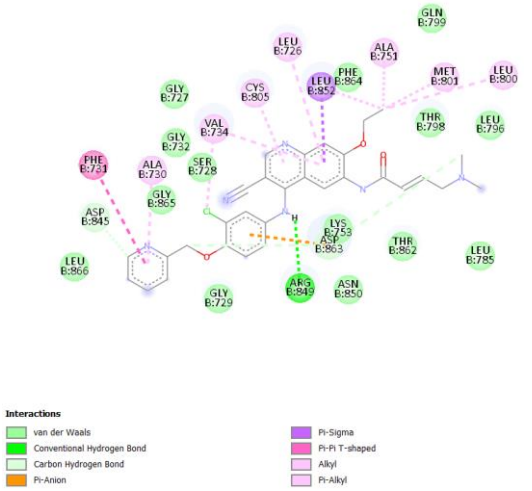

Rank 7:
Neratinib docked residue

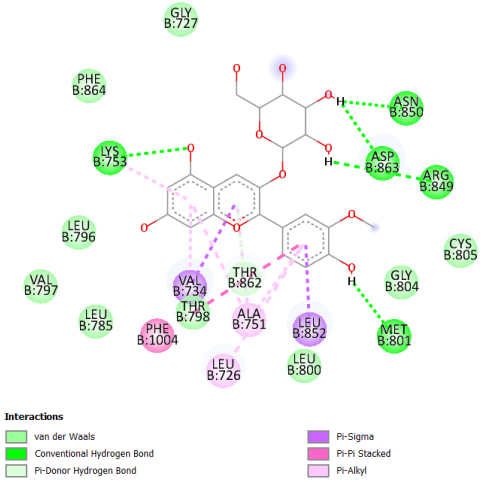

Rank 8:
Peonidin-3-glucoside docked residue

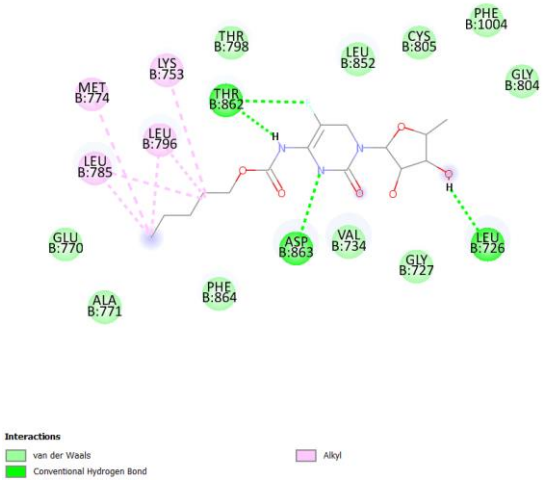

Rank 9:
Capecitabine docked residue

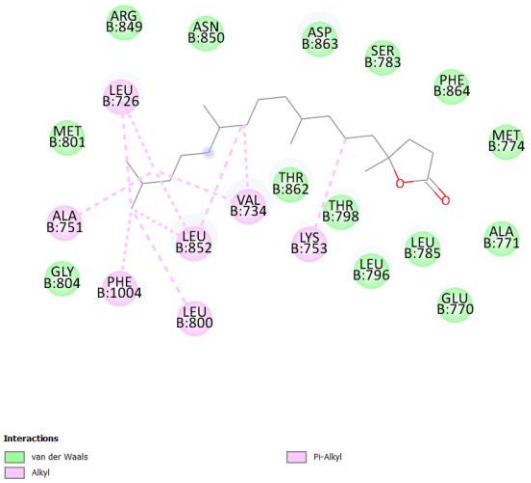

Rank 10:
4,8,12,16-tetramethylheptadecan-4-olide docked residue

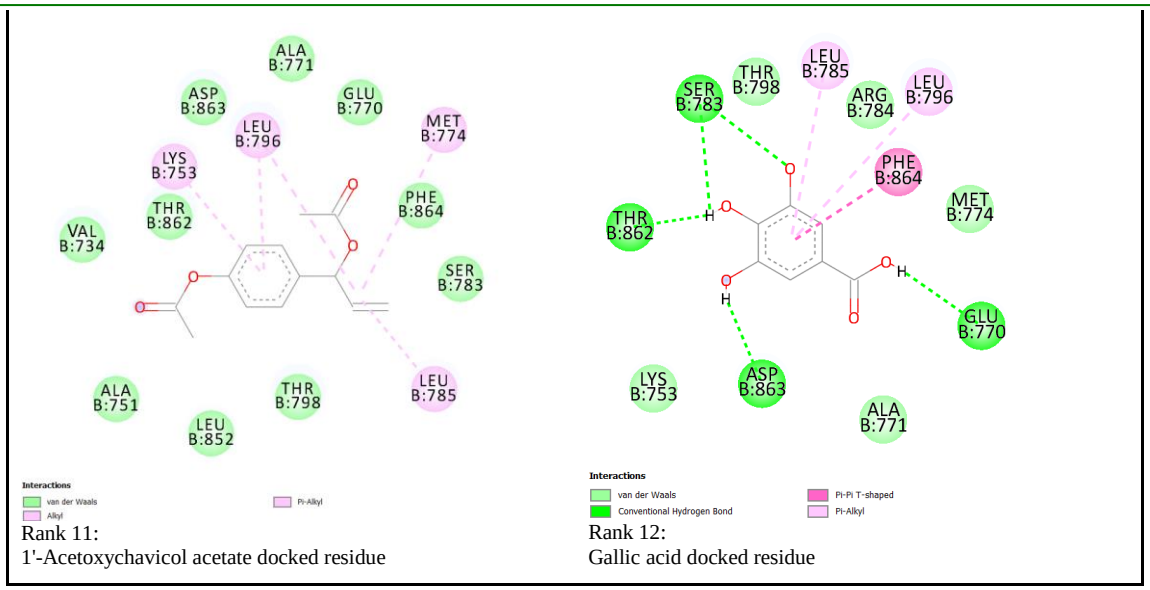

Figure 6. Visualization of HER2in binding residues with control SYR127063, approved inhibitor, and plant-based inhibitor, as well as BIOVIA visualization of 3PP0.

According to Figure 6, a total of 14 visualized interaction types, compromising of van der Waals, water hydrogen bond, conventional hydrogen bond, carbon-hydrogen bond, halogen (Cl, Br, I), halogen (fluorine), Pi-donor hydrogen bond, Pi-Sigma, Pi-Pi T-shaped, Pi-Pi stacked, alkyl, Pi-alkyl, and Pi-anion. Overall, the HER2in subdomain II's binding groove's amino acids that interact with ligands are numbered around the 727-864th amino acids and a 1004th amino acid.

Visualized control SYR127063 from 3PP0 shows 29 residue interactions and 11 types compared to the control SYR127063 from docking having 25 residue interactions and 9 types. The 3PP0 crystal structure was obtained from a wet lab model using X-ray diffraction illustrates a more specific and broader array of interactions compared to molecular docking software. Although, upon comparing the interactions, it still exhibits interaction in similar locations. In addition, as seen in Leu785, the residue type of interaction changes from alkyl to Pi-sigma, indicating that molecular docking software does not show an exact 100% result, which may apply to other ligands as well.

As for Tucatinib, it previously had greater binding affinity than Lapatinib, however, Lapatinib has 25 residue interactions and 9 types, while Tucatinib has 23 residue interactions and 6 types. Lapatinib interacts with HER2 receptors through Lys724, Leu726, Val734, Lys736, Ala751, Lys753, Ser783, Leu785, Leu796, Thr798, Met801, Pro802, Gly804, Cys805, Asp808, Leu852, Thr862, and Asp863 amino acid residues. Lys736 and Pro802 are involved in hydrogen bonding, whereas Lys724 is important in forming hydrogen bonds with ligands, especially the more hydrogen bonds, a higher inhibition activity occurs. Thr798, Leu852, Val734, and Gly804 are involved in hydrophobic interaction, Asp863 and Lys724 showed electrostatic interactions, and Phe864, Thr798, Ser783, and Met801 showed Van der Waals interactions. Cys805, Lys753, and Leu796 are involved in Pi-alkyl interactions, and Leu726 is involved in Pi-sigma interactions (Sohrab and Kamal, 2022).

Meanwhile, plant-based inhibitor Coptisine has 16 residue interactions and 5 types, while Sanguinarine has 12 residue interactions and 6 types. Even though Coptisine has more residue interactions than Sanguinarine, Sanguinarine has an additional form of residue interaction of Pi donor hydrogen bonds by aiding other interactions, which is great for inhibition activity as it enhances the binding affinity and overall stability of the protein-ligand complex, thus, raising Sanguinarine's potential as an HER2in inhibitor

Molecular dynamics of ligand-HER2in stability analysis

The conducted molecular dynamics simulations using CABSflex 2.0, is a fast-modeling tool designed to simulate biomolecular stability and movements efficiently. This tool utilizes the CABS model, a recognized coarse-grained protein modeling approach capable of producing protein dynamics at minimal computational cost, promote enhanced features, such as the ability to process larger proteins, customizable simulation parameters, and contact map generation, as well as insights into protein stability through the RMSF plot (Aurora et al., 2022). The analysis primarily focused on the stability of each ligand binding to the protein HER2in, as indicated by RMSF values of armstrong (Å) that should lie in the range lower than 2Å which indicate a residue conformation relatively stable during simulations (Pawara et al., 2021), especially in the binding site for a stabler protein-ligand binding (Ejaz et al., 2023). Not only lower armstrong values, symmetrical fluctuations also contribute to greater stability compared to unsymmetrical fluctuation (Vishvakarma et al., 2022), typically 1-3Å fluctuations is the acceptable range according to Aurora et al. (2023). Greater stability in atomic movements within protein-ligand complex corresponded to improved prediction accuracy and more reliable results (Aurora et al., 2023; Khan et al., 2024).

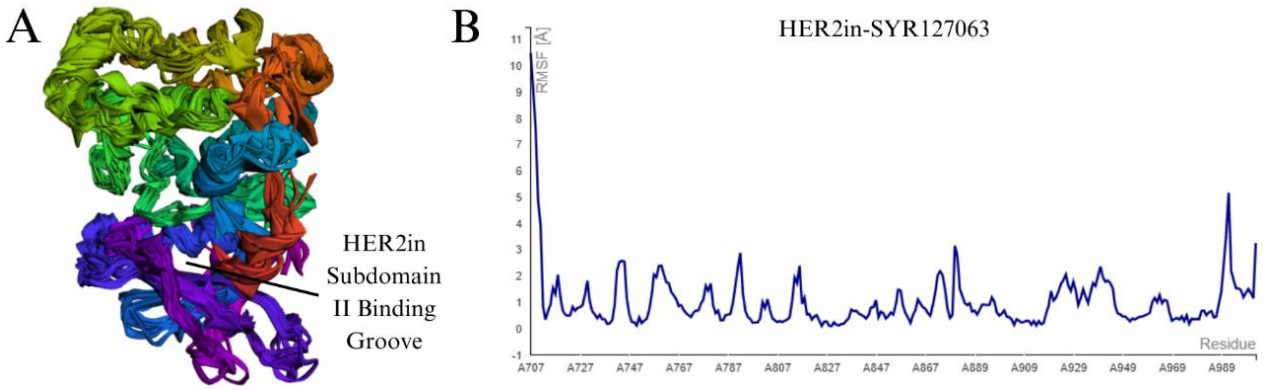

Figure 7. Molecular dynamics simulation of control ligand and its interactors. The molecular model structure of 3PP0 HER2in domain II and control ligand SYR127063 (A). The RMSF plot of 3PP0 and control ligand SYR127063 (B).

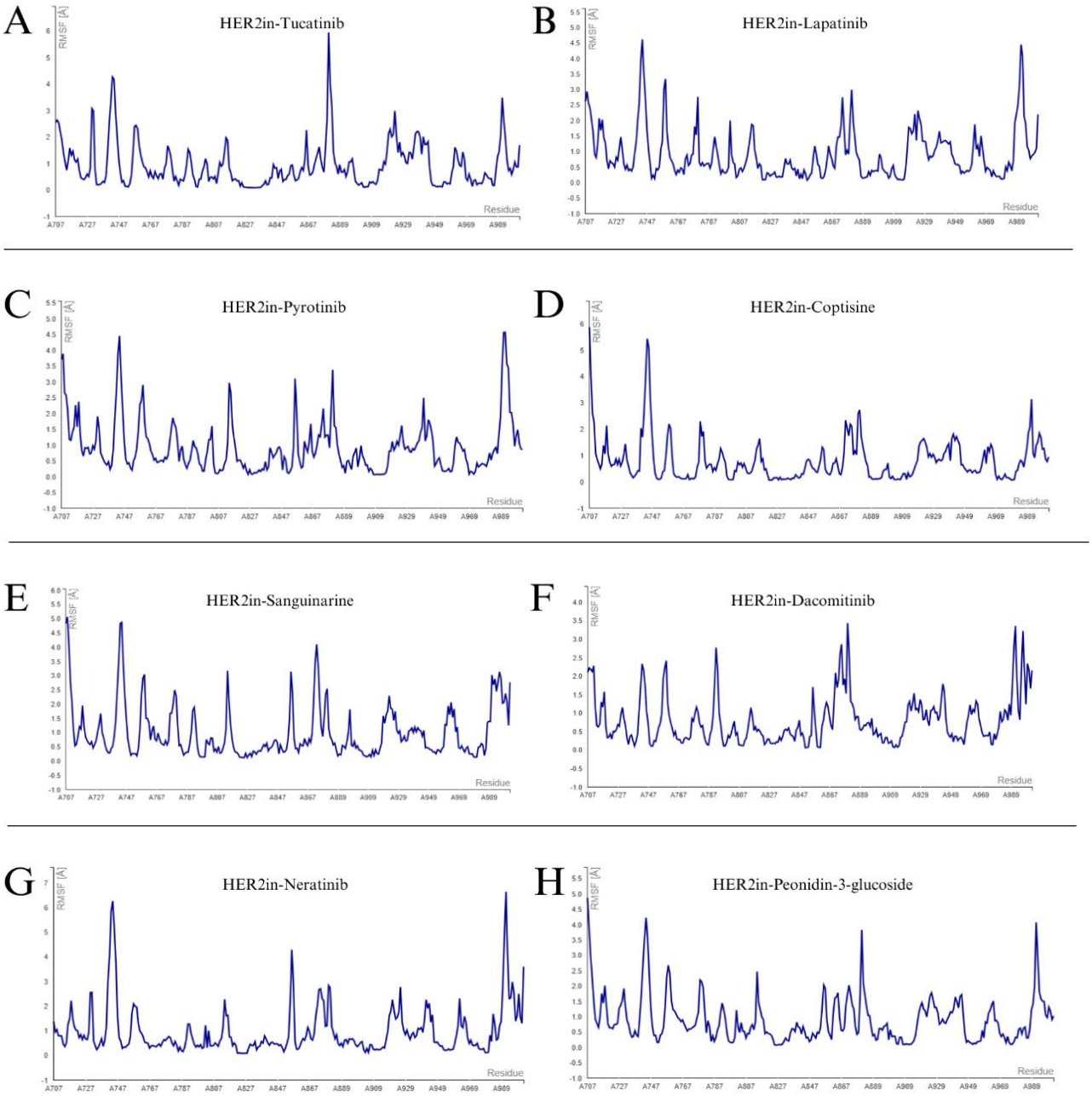

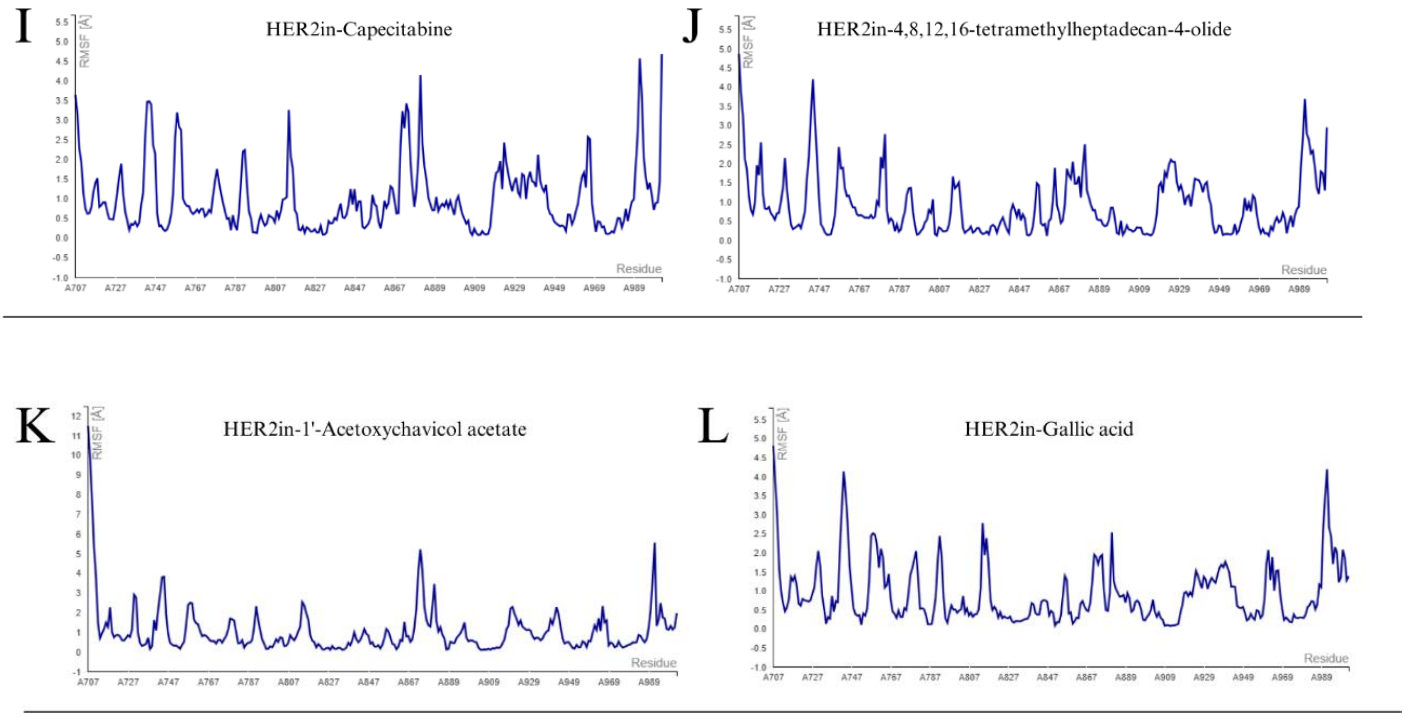

Figure 8. Molecular dynamics simulation of approved and plant-based ligands' interactors. The RMSF plot of 3PP0 HER2in domain II and Tucatinib (A), Lapatinib (B), Pyrotinib (C), Coptisine (D), Sanguinarine (E), Dacomitinib (F), Neratinib (G), Peonidin-3-glucoside (H), Capecitabine (I), 4,8,12,16-Tetramethylheptadecan-4-olide (J), 1'-Acetoxychavicol acetate (K) and Gallic Acid (L).

The molecular dynamics results (Figure 7 and 8) demonstrate overall stability across the interactions between all ligands and HER2in subdomain II receptors, which exhibited nearly around 70-90 % of atomic fluctuations remaining below 3Å (Aurora et al., 2023; Khan et al., 2024), while 3 peaks in Coptisine, Dacomitinib, Neratinib, Peonidin-3-glucoside, 4,8,12,16-Tetramethylheptadecan-4-olide, and Gallic Acid; 4 peaks in Tucatinib, and Lapatinib; 5 peaks only in 1'-Acetoxychavicol acetate; 7 peaks in Pyrotinib and Sanguinarine; and 8 peaks in Capecitabine with more than equal 3Å was shown in the respective RMSF plots. Although it is worth noting that some of the peaks barely pass 3Å threshold, however still considered as above 3Å peaks. In comparison to the control SYR127063 ligand with only 2 peaks above 3Å, which is the most stable, RMSF plots with 3 and 4 peaks above 3Å is considered as stable and moderately stable, while furthermore of 5 to 8 peaks are unstable.

Upon in depth assessment using Discovery Studio BIOVIA protein-ligand binding interaction results (refer to Figure 6) to address Ejaz et al. (2023) and Pawara et al. (2021) parameter of stable RMSF plot, the amino acid range that participates in the protein-ligand binding groove are 727-864th amino acids and an additional 1004th amino acid of HER2in subdomain II. Within the binding groove, the violation of above than 3Å peaks are not identified in SYR127063 and Dacomitinib, while the rest have around 1 or 2. A major percentage of Å's values are lower than 2Å are seen in Coptisine, Dacomitinib, Neratinib and Peonidin-3-glucoside, and around a total of six to ten peak symmetrical fluctuations are seen in the ligands' RMSF plots within the binding groove. Overall, suggesting that approved inhibitor Dacomitinib has the highest stability, followed by Coptisine, Neratinib and Peonidin-3-glucoside toward HER2in subdomain II, serving these as promising candidates for HER2in inhibitors according to their protein-ligand stability

Lipinski's Rule of Five

Lipinski's Rule of Five is a set of guidelines used to assess the drug-likeness of molecules, providing predictive insights into their potential success or failure in drug development. This rule is based on the understanding that orally effective drugs are typically small, moderately lipophilic compounds with specific physicochemical properties that influence pharmacokinetics. Biosimilars of Trastuzumab and Pertuzumab are not included in Lipinski's Rule of Five tests. The rule consists of five key criteria: a molecular weight of less than 500 Dalton (Da), a partition coefficient (LogP) of less than 5, fewer than 5 hydrogen donors, fewer than 10 hydrogen acceptors, and a molar refractivity between 40 and 130. These criteria ensure that the compound has optimal solubility and membrane permeability for acceptable absorption and bioavailability as an orally active drug in humans (Roskoski, 2019; Tijjani et al., 2022). Violations of two or more of these criteria typically indicate potential issues with absorption and overall bioavailability, which may impair the compound's efficacy as a drug. Therefore, an orally active drug should not have more than one violation of Lipinski's Rule of Five criteria (Kumar et al., 2022).

Table 4. Lipinski's Rule of Five Analysis

Chemical ligand name	Molecular Weight (g/mol)	H-bonds donors /acceptors	Consensus Lipophilicity (logP)	Lipinski Potential violations
Tucatinib	480.52	2/7	3.91	
Lapatinib	581.06	2/8	5.13	(MW>500)
Pyrotinib	583.092	2/7	4.59	(MW>500)
Coptisine	320.324	0/4	2.40	
Sanguinarine	332.335	0/4	2.88	
Dacomitinib	469.948	2/6	4.29	
Neratinib	557.054	2/7	4.24	(MW>500)
Peonidin-3-glucoside	301.274	4/6	0.97	
Capecitabine	359.354	3/8	0.75	
4,8,12,16-tetramethylheptadecan-4-olide	324.549	0/2	6.16	(MLOGP> 4.15)
1'-Acetoxychavicol acetate	234.251	0/4	2.39	
Gallic acid	170.12	4/5	0.21	

As reflected in Table 4, compounds Lapatinib, Pyrotinib, and Neratinib violate the molecular weight criterion by having a molecular weight of 581.06 Da, 583.092 Da, and 557.054 Da, respectively, which may affect their absorption and overall availability. Compound 4,8,12,16-Tetramethylheptadecan-4-olide violates the lipophilicity criterion by having a partition coefficient (LogP) of 6.16, indicating poor aqueous solubility and potential issues with absorption. Therefore, the compounds Tucatinib, Coptisine, Sanguinarine, Dacomitinib, Neratinib, Peonidin-3-glucoside, Capecitabine, 1'-Acetoxychavicol acetate, and Gallic Acid which meets all five of Lipinski's criteria demonstrate favorable drug-likeness profiles.

ADMET profiling

The choice of a chemical ligand inhibitor should be based on the following ADMET parameter (Arsianti et al., 2023; El-Saadi et al., 2015; Tung et al., 2023).

Table 5. Ligand inhibitor ADMET analysis

No	Compound name and molecular weight	Absorption	Distribution	Metabolism	Excretion	Toxicity
		CACO3 permeability (log Papp in 10^{-6} cm/s), **Intestinal absorption**	**VDss** (Log L/kg)	**CYP2D6 substrate, CYP3A4 substrate, CYP2D6 inhibitor, CYP3A4 inhibitor**	**Total clearance** (log ml/min/kg)	**AMES toxicity, Hepatotoxicity**
1	Lapatinib (581.1 g/mol)	0.628, 100%	-0.175	No, Yes, No, Yes	0.659	No, Yes
2	Tucatinib (480.5 g/mol)	1.669, 100%	0.351	No, Yes, No, Yes	0.487	No, Yes
3	Pyrotinib (583.1g/mol)	1.21, 92.289%	1.565	No, Yes, No, Yes	0.841	No, Yes
4	Neratinib (557 g/mol)	0.898, 86.975%	1.392	No, Yes, No, Yes	0.743	No, Yes
5	Dacomitinib (469.9 g/mol)	0.991, 89.104%	1.292	Yes, Yes, No, Yes	0.695	No, Yes
6	Capecitabine (359.35 g/mol)	0.174, 61.439%	-0.205	No, No, No, No	1.049	No, Yes
7	4,8,12,16-Tetramethylheptadecan-4-olide (324.5 g/mol)	1.613, 92.444%	0.412	No, Yes, No, No	1.151	No, No
8	1'-Acetoxychavicol acetate (234.25 g/mol)	1.305, 95.801%	-0.225	No, No, No, No	0.56	No, No
9	Gallic acid (170.12 g/mol)	-0.043, 37.554%	-1.885	No, No, No, No	0.569	No, No
10	Peonidin-3-glucoside (463.4 g/mol)	-0.507, 42.62%	-0.334	No, No, No, No	0.886	No, No
11	Coptisine (320.3 g/mol)	1.752, 100%	0.862	No, Yes, Yes, Yes	1.289	Yes, Yes
12	Sanguinarine (332.3 g/mol)	1.249, 99.961	1.068	No, Yes, Yes, Yes	1.068	Yes, No

A substance is considered poorly absorbed if the percentage absorbed in the human intestine is less than 30%. By referring to Table 5, the best compounds Lapatinib, Tucatinib, Sanguinarine, and Coptisine show around 90% to 100% absorption. A compound has high Caco-2 permeability if it has log Papp > 0.9. Tucatinib, Coptisine, and Sanguinarine show a high Caco-2 permeability. The higher the VDss, the more the drug is distributed in tissue rather than plasma. Well distributed to tissues if logVDss > 0.45 and poorly distributed if logVDss < -0.15. Tucatinib and Lapatinib show poor distribution to tissue, while Coptisine and Sanguinarine show great distribution to tissues. The cytochrome P450 plays an important role in the metabolism of many drugs, and metabolism will be based on CYP2D6 and CYP3A4 substrate, CYP2D6 and CYP3A4 inhibitors. P450 inhibitors can significantly alter the pharmacokinetics of these drugs. Enzyme inhibition reduces metabolism, whereas induction increases it. According to this, Tucatinib and Lapatinib have greater metabolism efficiency due to Sanguinarine and Coptisine inhibiting both CYP2D6 and CYP3A4. Elimination is based on total clearance. Coptisine and Sanguinarine show a higher clearance rate compared to Lapatinib and Tucatinib, which means it is highly effective at removing drugs from circulation. Toxicity is based on AMES toxicity and Hepatotoxicity. Lapatinib and Tucatinib do not cause carcinogenic effects (AMES toxicity), while Sanguinarine and Coptisine do. Sanguinarine does not cause liver (hepatotoxicity) damage, while the other

does. Interestingly, 4,8,12,16-Tetramethylheptadecan-4-olide, 1'-Acetoxychavicol acetate, Gallic Acid, and Peonidin-3-glucoside does not cause both AMES- and hepato-toxicity. Overall, Sanguinarine can be considered the best compound, even though it may induce carcinogenic effects, it can be eliminated faster to show less effect as shown from the elimination value, which means less interaction between cells. Biosimilars of Trastuzumab and Pertuzumab are not included in the ADMET profiling test.

HER2 functional protein-protein partners

HER2 or ERBB2, has numerous functional protein partners such as EGF, ERBB3, EGFR, NRG1, HSP90AA1, ERBB4, SRC, GRB2, CD44, and SHC1, which achieve over 0.999 score that means how high the fidelity of their interactions with HER2.

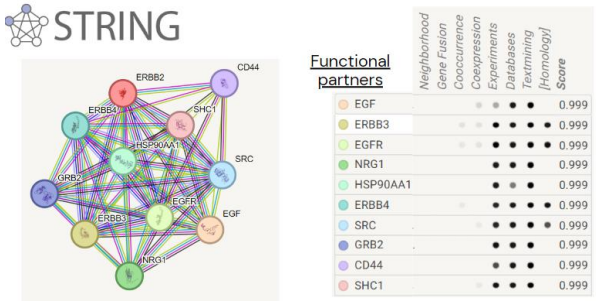

Figure 9. HER2 protein-protein partners

EGF and EGFR are well known for their role in cell proliferation and survival. The interaction between HER2 and EGFR is crucial in activating downstream signaling pathways, such as the PI3K/AKT and MAPK pathways, essential for cellular growth and differentiation (Stefani et al., 2021). By referring to Figure 9, there are several functional protein partners of HER2 (ERBB2), such as EGF, ERBB3, EGFR, NRG1, HSP90AA1, ERBB4, SRC, GRB2, CD44, and SHC1 with interaction scores over 0.999 denote the robustness and fidelity of these interactions, underscoring their biological significance. HER2's interaction with other ERBB family members, including ERBB3 and ERBB4, further amplifies its signaling capacity. The dimerization of HER2 and ERBB3 is particularly significant in activating PI3K/AKT signaling, which is crucial for tumorigenesis. NRG1 acts as a ligand for ERBB3 and ERBB4, facilitating the formation of active HER2-ERBB3 or HER2-ERBB4 heterodimers, indicating a significant role in mediating oncogenic signaling (Pamidiboina, 2020).

On the other hand, HSP90AA, a chaperone protein, stabilizes many proteins, including HER2, suggesting that HSP90AA1 is critical for maintaining the stability and functional conformation of HER2. This interaction also provides a therapeutic target, as HSP90 inhibitors can lead to the degradation of HER2, offering a strategic approach to cancer treatment (Greither, 2020). SRC and GRB2 are key components in signal transduction pathways, promoting cell proliferation survival and linking receptor tyrosine kinases to the Ras signaling pathway (Wang et al., 2024). CD44, involved in cell-cell interactions, adhesion, and migration, and SHC1, an adaptor protein in signaling pathways downstream of receptor tyrosine kinases, both enhance oncogenic signaling and promote tumor progression (Hassan and Seno, 2022).

Limitations

The limitation of this research includes the unavailability of ClusPro 2.0 and PDBsum ID (vpo7, vpo8, vpo9, and vpp1) antibody-receptor docking data of which has been expired or auto-deleted by the website as months from the docking date has passed. ClusPro 2.0 docking run results in cannot be run in CABSflex 2.0 due to the error of "AttributeError: 'NoneType' object has no attribute 'replica'". ClusPro 2.0 changes the attribute of some chains in vpo7 and vpo8 into another chain (e.g., heavy chain becomes HER2ex's chain).

Conclusion

In conclusion, the choice of extracellular antibody should be in the form of an antibody that has a wide array of residue interactions. 4HJG (improved Trastuzumab) and control Pertuzumab docked with HER2ex show the best binding affinity compared to control Trastuzumab and 4LLW (improved Pertuzumab), denoted as the best extracellular antibody due to it requiring much less energy to bind. However, 4LLW showed more ubiquitous residue interactions. This goes the same as 4HJG. As for intracellular ligand inhibitors, Lapatinib and Tucatinib require much less binding energy meaning higher binding affinity to extracellular HER2 compared to control and plant-based inhibitors. However, there are noteworthy plant-based inhibitors for Coptisine and Sanguinarine that have minuscule differences with the control's binding affinity value. Protein-ligand stability analysis results show that Dacomitinib has the highest stability, followed by Coptisine, Neratinib and Peonidin-3-glucoside. Lipinski's Rule of Five, ADMET profile screening, and Molecular Docking results have shown Sanguinarine to be the best compound that is derived from plants, while the approved inhibitor is Lapatinib. Although Lapatinib violates MW>500 Lipinski drug likeness parameters, and Sanguinarine's protein-ligand stability analysis proved unstable. Upon the inhibition of HER2, the other protein partners of HER2 that require interaction with HER2 to facilitate further proliferation mechanisms will also be downregulated. These results require future studies of *in vitro* cell-based assays to test the efficacy of the plant-based inhibitors toward HER2 receptor activity compared to the control inhibitors, and its cellular safety through MTS assay.

Acknowledgement

The authors would like to praise God, the Almighty, for providing us the opportunity and capability to accomplish this research paper. We would like to thank the Department of Research and Community Service (LPPM) of Indonesia International Institute for Life Sciences (i3L) for their heartfelt support.

References

Akinnusi, P. A., Olubode, S. O., Adebesin, A. O., Nana, T. A., & Shodehinde, S. A. (2022). Discovery of Promising Inhibitors of Epidermal Growth Factor Receptor (EGFR), Human Epidermal Growth Factor Receptor 2 (HER2), Estrogen Receptor (ER), and Phosphatidylinositol-3-kinase a (PI3Ka) for Personalized Breast Cancer Treatment. *Cancer Informatics*, *21*, 117693512211278. https://doi.org/10.1177/11769351221127862

Alifiansyah, M. R. T., Herdiansyah, M. A., Pratiwi, R. C., Pramesti, R. P., Hafsyah, N. W., Rania, A. P., Putra, Ju. E. R. P., Cahyono, P. A., Litazkiyyah, Muhammad, S. K., Murtadlo, A. A. A., Kharisma, V. D., Ansori, A. N. M., Jakhmola, V., Ashok, P. K., Kalra, J. M., Purnobasuki, H., & Pratiwi, I. A. (2024). QSAR of acyl alizarin red biocompound derivatives of Rubia tinctorum roots and its ADMET properties as anti-breast cancer candidates against MMP-9 protein receptor: In Silico study. *Food Systems*, *7*(2), 312–320. https://doi.org/10.21323/2618-9771-2024-7-2-312-320

Ansori, A. N. M., Widyananda, M. H., Antonius, Y., Murtadlo, A. A. A., Kharisma, V. D., Wiradana, P. A., ... & Zainul, R. (2024). A review of cancer-related hypercalcemia: Pathophysiology, current treatments, and future directions. *Journal of Medicinal and Pharmaceutical Chemistry Research*, *6*(7), 944-952.

Arienti, C., Pignatta, S., & Tesei, A. (2019). Epidermal Growth Factor Receptor Family and its Role in Gastric Cancer. *Frontiers in Oncology*, *9*, 1308. https://doi.org/10.3389/fonc.2019.01308

Arsianti, A., Azizah, N. N., & Erlina, L. (2023). Molecular docking, ADMET profiling of Gallic Acid and its derivatives (N-alkyl gallamide) as apoptosis agent of breast cancer MCF-7 Cells. *F1000Research*, *11*, 1453–1453. https://doi.org/10.12688/f1000research.127347.2

Aurora, Y., Tarigan, I. P. N., Suryanto, N. M. M., Santosa, P., Pricillia, V., & Parikesit, A. A. (2022). Identification of flavonoids of Kalanchoe Pinnata as candidate drugs for COVID-19 gamma-variant treatment. *Malaysian Journal of Fundamental and Applied Sciences*, *18*(6), 630-643.

Boix-Perales, H., Borregaard, J., Jensen, K. B., Ersbøll, J., Galluzzo, S., Giuliani, R., Ciceroni, C., Melchiorri, D., Salmonson, T., Bergh, J., Schellens, J. H., & Pignatti, F. (2014). The European Medicines Agency Review of Pertuzumab for the treatment of adult patients with HER2-Positive Metastatic or locally recurrent unresectable breast cancer: Summary of the Scientific Assessment of the Committee for Medicinal Products for Human Use. *The Oncologist*, *19*(7), 766–773. https://doi.org/10.1634/theoncologist.2013-0348

Burley, S. K., Berman, H. M., Duarte, J. M., Feng, Z., Flatt, J. W., Hudson, B. P., Lowe, R., Peisach, E., Piehl, D. W., Rose, Y., Sali, A., Sekharan, M., Shao, C., Vallat, B., Voigt, M., Westbrook, J. D., Young, J. Y., & Zardecki, C. (2022). Protein Data Bank: A Comprehensive Review of 3D Structure Holdings and Worldwide Utilization by Researchers, Educators, and Students. *Biomolecules*, 12(10), 1425. https://doi.org/10.3390/biom12101425

Cavallaro, P. A., Santo, M. D., Belsito, E. L., Longobucco, C., Curcio, M., Morelli, C., Pasqua, L., & Leggio, A. (2023). Peptides Targeting HER2-Positive Breast Cancer Cells and Applications in Tumor Imaging and Delivery of Chemotherapeutics. *Nanomaterials*, *13*(17), 2476–2476. https://doi.org/10.3390/nano13172476

Che, X., Liu, Q., & Zhang, L. (2023). An accurate and universal protein-small molecule batch docking solution using Autodock Vina. *Results in Engineering*, *19*, 101335. https://doi.org/10.1016/j.rineng.2023.101335

Collins, D. M., Conlon, N. T., Kannan, S., Verma, C. S., Eli, L. D., Lalani, A. S., & Crown, J. (2019). Preclinical Characteristics of the Irreversible Pan-HER Kinase Inhibitor Neratinib Compared with Lapatinib: Implications for the Treatment of HER2-Positive and HER2-Mutated Breast Cancer. *Cancers*, *11*(6), 737. https://doi.org/10.3390/cancers11060737

Cordover, E., & Minden, A. (2020). Signaling pathways downstream to receptor tyrosine kinases: targets for cancer treatment. *Journal of Cancer Metastasis and Treatment*, *2020*. https://doi.org/10.20517/2394-4722.2020.101

Cruz, V. L., Souza-Egipsy, V., Gión, M., Pérez-García, J. M., Cortés, J., Ramos, J., & Vega, J. F. (2023). Binding Affinity of Trastuzumab and Pertuzumab Monoclonal Antibodies to Extracellular HER2 Domain. *International Journal of Molecular Sciences*, *24*(15), 12031–12031. https://doi.org/10.3390/ijms241512031

Deepasree, K., & Subhashree, V. (2023). Molecular docking and dynamic simulation studies of terpenoid compounds against phosphatidylinositol-specific phospholipase C from Listeria monocytogenes. *Informatics in Medicine Unlocked*, *39*, 101252. https://doi.org/10.1016/j.imu.2023.101252

Desta, I. T., Kotelnikov, S., Jones, G., Ghani, U., Abyzov, M., Kholodov, Y., Standley, D. M., Beglov, D., Vajda, S., & Kozakov, D. (2023). The ClusPro AbEMap web server for the prediction of antibody epitopes. *Nature Protocols*, *18*(6), 1814–1840. https://doi.org/10.1038/s41596-023-00826-7

Dibha, A., Wahyuningsih, S., Ansori, A., Kharisma, V., Widyananda, M., Parikesit, A., Sibero, M., Probojati, R., Murtadlo, A., Trinugroho, J., Sucipto, T., Turista, D., Rosadi, I., Ullah, M., Jakhmola, V., & Zainul, R. (2022). Utilization of Secondary Metabolites in Algae Kappaphycus alvarezii as a Breast Cancer Drug with a Computational Method. *Pharmacognosy Journal*, *14*(3), 536–543. https://doi.org/10.5530/pj.2022.14.68

Ejaz, S. A., Aziz, M., Zafar, Z., Akhtar, N., & Ogaly, H. A. (2023). Revisiting the inhibitory potential of protein kinase inhibitors against NEK7 protein via comprehensive computational investigations. *Scientific Reports*, *13*(1). https://doi.org/10.1038/s41598-023-31499-7

El-Saadi, M. W., Williams-Hart, T., Salvatore, B. A., & Mahdavian, E. (2015). Use of in-silico assays to characterize the ADMET profile and identify potential therapeutic targets of fusarochromanone, a novel anti-cancer agent. *In Silico Pharmacology*, *3*(1). https://doi.org/10.1186/s40203-015-0010-5

Gaibar, M., Beltrán, L., Romero-Lorca, A., Fernández-Santander, A., & Novillo, A. (2020). Somatic Mutations in HER2 and Implications for Current Treatment Paradigms in HER2-Positive Breast Cancer. *Journal of Oncology*, *2020*, 1–13. https://doi.org/10.1155/2020/6375956

Galogre, M. I., Rodin, D., Pyatnitskiy, M. A., Mackelprang, M., & Koman, I. (2023). A review of HER2 overexpression and somatic mutations in cancers. *Critical Reviews in Oncology/Hematology*, *186*, 103997–103997. https://doi.org/10.1016/j.critrevonc.2023.103997

Goutsouliak, K., Veeraraghavan, J., Sethunath, V., De Angelis, C., Osborne, C. K., Rimawi, M. F., & Schiff, R. (2019). Towards personalized treatment for early stage HER2-positive breast cancer. *Nature Reviews Clinical Oncology*, *17*(4), 233–250. https://doi.org/10.1038/s41571-019-0299-9

Greither, M. (2020). *Identification of a point mutation as a mechanism underlying HSP90 inhibitor resistance*. https://nbn-resolving.de/urn/resolver.pl?urn:nbn:de:bvb:91-diss-20200130-1462792-1-0

Hassan, G., & Seno, M. (2022). ERBB Signaling Pathway in Cancer Stem Cells. *Springer EBooks*, 65–81. https://doi.org/10.1007/978-3-031-12974-2_3

Hamami, S. M. A., Fai, M., Aththar, A. F., Zakaria, M. N. Z., Kharisma, V. D., Mutardio, A. A. A., Tamam, M. B., … & Fitri, E. (2022). Nano Transdermal Delivery Potential of Fucoidan from Sargassum sp. (Brown Algae) as Chemoprevention Agent for Breast Cancer Treatment. *Pharmacognosy Journal*, *14*(6), 789–795. https://doi.org/10.5530/pj.2022.14.169

Herdiansyah, M. A., Ansori, A. N. M., Kharisma, V. D., Alifiansyah, M. R. T., Anggraini, D., Priyono, Q. A. P., ... & Maksimiuk, N. (2024). In Silico Study of Cladosporol and Its Acyl Derivatives as Anti-Breast Cancer Againts Alpha-Estrogen Receptor. *Biosaintifika: Journal of Biology & Biology Education*, *15*(1).

Hermanto, S., Yusuf, M., Mutalib, A., & Hudiyono, S. (2017). Molecular dynamic simulation of Trastuzumab F(ab')$_2$structure in corporation with HER2 as a theranostic agent of breast cancer. *Journal of Physics. Conference Series*, *835*, 012005–012005. https://doi.org/10.1088/1742-6596/835/1/012005

Jakhmola, V., Parashar, T., Ghildiyal, P., Ansori, A., Sharma, R. K., Rao, N. G. R., Kalra, K., Singh, N., Nainwal, N., Singh, R. K., Singh, M. P., Kimothi, V., Bhatt, A., Dimri, A., Kumar, R., Semwal, A., Aini, N. S., & Rebezov, M. (2022). An in

Silico study to explore the role of EGFR in ovarian cancer. *Pharmacognosy Journal*, *14*(6), 817–821. https://doi.org/10.5530/pj.2022.14.173

Kanthala, S., Mill, C. P., Riese, D. J., Jaiswal, M., & Jois, S. (2016). Expression and purification of HER2 extracellular domain proteins in Schneider2 insect cells. *Protein Expression and Purification*, *125*, 26–33. https://doi.org/10.1016/j.pep.2015.09.001

Khan, A. a. S., Yousaf, M. A., Azhar, J., Maqbool, M. F., & Bibi, R. (2024). Repurposing FDA approved drugs against monkeypox virus DNA dependent RNA polymerase: virtual screening, normal mode analysis and molecular dynamics simulation studies. *VirusDisease*, *35*(2), 260–270. https://doi.org/10.1007/s13337-024-00869-8

Kozakov, D., Hall, D. R., Xia, B., Porter, K. A., Padhorny, D., Yueh, C., Beglov, D., & Vajda, S. (2017). The ClusPro web server for protein–protein docking. *Nature Protocols*, *12*(2), 255–278. https://doi.org/10.1038/nprot.2016.169

Kumar, D. T., Shree Devi, M. S., Kumar, S. U., Sherlin, A., Mathew, A., Lakshmipriya, M., Sathiyarajeswaran, P., Gnanasambandan, R., Siva, R., Magesh, R., & George Priya Doss, C. (2022). Understanding the activating mechanism of the immune system against COVID-19 by Traditional Indian Medicine: Network pharmacology approach. *Advances in Protein Chemistry and Structural Biology*, 275–379. https://doi.org/10.1016/bs.apcsb.2021.11.007

Kumar, R., George, B., Campbell, M. R., Verma, N., Paul, A. M., Melo-Alvim, C., Ribeiro, L., Pillai, M. R., da Costa, L. M., & Moasser, M. M. (2020). HER family in cancer progression: From discovery to 2020 and beyond. *Advances in Cancer Research*, 109–160. https://doi.org/10.1016/bs.acr.2020.04.001

Murthy, R., Borges, V. F., Conlin, A., Chaves, J., Chamberlain, M., Gray, T., Vo, A., & Hamilton, E. (2018). Tucatinib with Capecitabine and Trastuzumab in advanced HER2-positive metastatic breast cancer with and without brain metastases: a non-randomised, open-label, phase 1b study. *The Lancet Oncology*, *19*(7), 880–888. https://doi.org/10.1016/s1470-2045(18)30256-0

Pamidiboina, V. (2020). *Molecular changes in EGFR downstream signalling and intracellular calcium changes associated with the cisplatin-resistant phenotype of lung cancer cells*. https://doi.org/10.5282/edoc.26397

Pantsar, T., & Poso, A. (2018). Binding Affinity via Docking: Fact and Fiction. *Molecules*, *23*(8), 1899. https://doi.org/10.3390/molecules23081899

Parikesit, A. A., Ansori, A. N. M., & Kharisma, V. D. (2024). Computational design of siRNA targeting Homo sapiens HER2 splice variant mRNA: A potential strategy for breast cancer intervention. *Biosaintifika Journal of Biology & Biology Education*, *16*(3). https://doi.org/10.15294/biosaintifika.v16i3.3685

Paul, J. K., Azmal, M., Shohan, M. N. H., Mrinmoy, M., Haque, A. S. N. B., Talukder, O. F., & Ghosh, A. (2025). Identification of natural phytochemicals as AKT2 inhibitors using molecular docking and dynamics simulations as potential cancer therapeutics. *Heliyon*, e41897. https://doi.org/10.1016/j.heliyon.2025.e41897

Paul, R., Kasahara, K., Sasaki, J., Pérez, J. F., Matsunaga, R., Hashiguchi, T., ... & Tsumoto, K. (2024). Unveiling the affinity–stability relationship in anti-measles virus antibodies: a computational approach for hotspots prediction. *Frontiers in Molecular Biosciences*, 10, 1302737.

Pawar, S., Kulkarni, C., Gadade, P., Pujari, S., Kakade, S., Rohane, S. H., & Redasani, V. K. (2023). Molecular docking using different tools. *Asian Journal of Pharmaceutical Research*, 13(4), 292-296.

Pawara, R., Ahmad, I., Surana, S., & Patel, H. (2021). Computational identification of 2,4-disubstituted amino-pyrimidines as L858R/T790M-EGFR double mutant inhibitors using pharmacophore mapping, molecular docking, binding free energy calculation, DFT study and molecular dynamic simulation. *In Silico Pharmacology*, *9*(1). https://doi.org/10.1007/s40203-021-00113-x

Peng, K., Zheng, Y., Xia, W., & Mao, Z. (2023). Organometallic antitumor agents: targeting from biomolecules to dynamic bioprocesses. *Chemical Society Reviews*, *52*(8), 2790–2832. https://doi.org/10.1039/d2cs00757f

Perumal, P. C., Prabhakaran, P., Sundaram, S., Oirere, E., Palanirajan, A., Balu, V., Deivasigamani, M., Kannappan, P., Samynathan, R., & Gopalakrishnan, V. K. (2015). Discovery of Novel Inhibitors for HER2 from Natural Compounds Present in Cayratia trifolia (l.): An In silico Analysis. *International Journal of Current Pharmaceutical Review and Research*, *6*(3), 164–168.

Pradubyat, N., Giannoudis, A., Elmetwali, T., Mahalapbutr, P., Palmieri, C., Mitrpant, C., & Ketchart, W. (2021). 1′-Acetoxychavicol Acetate from Alpinia galanga Represses Proliferation and Invasion, and Induces Apoptosis via HER2-signaling in Endocrine-Resistant Breast Cancer Cells. *Planta Medica*, *88*(02), 163–178. https://doi.org/10.1055/a-1307-3997

Rahman, A. T., Rafia, R., Jethro, A., Santoso, P., Kharisma, V. D., Affan, A., Purnamasari, D., … & Sari. (2022). In Silico Study of the Potential of Endemic Sumatra Wild Turmeric Rhizomes (Curcuma Sumatrana: Zingiberaceae) As Anti-Cancer. *Pharmacognosy Journal*, *14*(6), 806–812. https://doi.org/10.5530/pj.2022.14.171

Raubenolt, B., & Blankenberg, D. (2024). Generalized open-source workflows for atomistic molecular dynamics simulations of viral helicases. *GigaScience*, 13, giae026.

Roskoski, R. (2019). Properties of FDA-approved small molecule protein kinase inhibitors. *Pharmacological Research*, *144*, 19–50. https://doi.org/10.1016/j.phrs.2019.03.006

Sohrab, S. S., & Kamal, M. A. (2022). Screening, Docking, and Molecular Dynamics Study of Natural Compounds as an Anti-HER2 for the Management of Breast Cancer. *Life (Basel, Switzerland)*, *12*(11), 1729. https://doi.org/10.3390/life12111729

Stefani, C., Miricescu, D., Stanescu-Spinu, I.-I., Nica, R. I., Greabu, M., Totan, A. R., & Jinga, M. (2021). Growth Factors, PI3K/AKT/mTOR and MAPK Signaling Pathways in Colorectal Cancer Pathogenesis: Where Are We Now? *International Journal of Molecular Sciences*, *22*(19), 10260. https://doi.org/10.3390/ijms221910260

Tijjani, H., Olatunde, A., Adegunloye, A. P., & Ishola, A. A. (2022). In silico insight into the interaction of 4-aminoquinolines with selected SARS-CoV-2 structural and nonstructural proteins. *Elsevier EBooks*, 313–333. https://doi.org/10.1016/b978-0-323-95578-2.00001-7

Trott, O., & Olson, A. J. (2009). AutoDock Vina: Improving the speed and accuracy of docking with a new scoring function, efficient optimization, and multithreading. *Journal of Computational Chemistry*, *31*(2), 455–461. https://doi.org/10.1002/jcc.21334

Tung, B. T., Son, N. N., Kim, N. B., Hong, T., & Minh, P. H. (2023). In silico screening of alkaloids as potential inhibitors of HER2 protein for breast cancer treatment. *Vietnam Journal of Chemistry*, *61*(3), 308–317. https://doi.org/10.1002/vjch.202200135

Vishvakarma, V. K., Singh, M. B., Jain, P., Kumari, K., & Singh, P. (2022). Hunting the main protease of SARS-CoV-2 by plitidepsin: Molecular docking and temperature-dependent molecular dynamics simulations. *Amino Acids*, *54*(2), 205–213. https://doi.org/10.1007/s00726-021-03098-1

Wang, D., Liu, G., Meng, Y., Chen, H., Ye, Z., & Jing, J. (2024). The Configuration of GRB2 in Protein Interaction and Signal Transduction. *Biomolecules*, *14*(3), 259. https://doi.org/10.3390/biom14030259

Wang, J., Zhang, B., Cheng, X., Li, Q., Lv, H., Nie, C., Chen, B., Xu, W., Zhao, J., He, Y., Tu, S., & Chen, X. (2022). Retrospective Study on the Efficacy and Safety of Pyrotinib-Based Therapy for HER2-Positive Nonbreast Advanced Solid Tumors. *Journal of Oncology*, *2022*, 1–8. https://doi.org/10.1155/2022/4233782

Widyananda, M. H., Pratama, S. K., Samoedra, R. S., Sari, F. N., Kharisma, V. D., Ansori, A. N. M., & Antonius, Y. (2021). Molecular docking study of sea urchin (Arbacia lixula) peptides as multi-target inhibitor for non-small cell lung cancer (NSCLC) associated proteins. *Journal of Pharmacy & Pharmacognosy Research*, *9*(4), 484–496. https://doi.org/10.56499/jppres21.1047_9.4.484

Yahaya, M. A. F., Bakar, A. A., Stanslas, J., Nordin, N., Zainol, M., & Mehat, M. Z. (2021). Insights from molecular docking and molecular dynamics on the potential of vitexin as an antagonist candidate against lipopolysaccharide (LPS) for microglial activation in neuroinflammation. *BMC biotechnology*, 21(1), 38.

Yang, G., Liu, R., & Tang, X. (2024). Dacomitinib exhibits promising activity against the rare HER2 exon 20 insertion M774delinsWLV in lung cancer: A case report and literature review. *Heliyon*, *10*(9), e30312–e30312. https://doi.org/10.1016/j.heliyon.2024.e30312

Zhang, H., Liu, Y., Liu, J., Chen, J., Wang, J., Hua, H., & Jiang, Y. (2024). cAMP-PKA/EPAC signaling and cancer: the interplay in tumor microenvironment. *Journal of Hematology & Oncology*, *17*, 5. https://doi.org/10.1186/s13045-024-01524-x

Zhang, Y., Wu, S., Zhuang, X., Weng, G., Fan, J., Yang, X., Xu, Y., Pan, L., Hou, T., Zhou, Z., & Chen, S. (2019). Identification of an Activating Mutation in the Extracellular Domain of HER2 Conferring Resistance to Pertuzumab. *OncoTargets and Therapy*, *Volume 12*, 11597–11608. https://doi.org/10.2147/ott.s232912

Zhao, J., Mohan, N., Nussinov, R., Ma, B., & Wu, W. J. (2021). Trastuzumab blocks the receiver function of HER2 leading to the population shifts of HER2-Containing homodimers and heterodimers. *Antibodies*, *10*(1), 7. https://doi.org/10.3390/antib10010007

Zhou, Q., Jin, P., Liu, J., Li, S., Liu, W., & Xi, S. (2021). Arsenic-induced HER2 promotes proliferation, migration and angiogenesis of bladder epithelial cells via activation of multiple signaling pathways in vitro and in vivo. *Science of the Total Environment*, *753*, 141962. https://doi.org/10.1016/j.scitotenv.2020.141962

Zimmer, A. S., Van Swearingen, A. E. D., & Anders, C. K. (2020). HER2-positive breast cancer brain metastasis: A new and exciting landscape. *Cancer Reports*. https://doi.org/10.1002/cnr2.1274